Quantum key distribution using quantum dot single-photon emitting diodes in the red and near infrared spectral range

2012 New J. Phys. 14 083001

(http://iopscience.iop.org/1367-2630/14/8/083001)

New Journal of Physics
The open-access journal for physics

Quantum key distribution using quantum dot single-photon emitting diodes in the red and near infrared spectral range

Tobias Heindel[1,6], Christian A Kessler[2,6], Markus Rau[3,6], Christian Schneider[1], Martin Fürst[3,4], Fabian Hargart[2], Wolfgang-Michael Schulz[2], Marcus Eichfelder[2], Robert Roßbach[2], Sebastian Nauerth[3,4], Matthias Lermer[1], Henning Weier[3,4], Michael Jetter[2], Martin Kamp[1], Stephan Reitzenstein[1,7], Sven Höfling[1,8], Peter Michler[2], Harald Weinfurter[3,5] and Alfred Forchel[1]

[1] Technische Physik and Wilhelm Conrad Röntgen Research Center for Complex Material Systems, Universität Würzburg, Am Hubland, 97074 Würzburg, Germany
[2] Institut für Halbleiteroptik und Funktionelle Grenzflächen, 70569 Stuttgart, Germany
[3] Fakultät für Physik, Ludwig-Maximilians-Universität, 80799 München, Germany
[4] qutools GmbH, 80539 München, Germany
[5] Max-Planck-Institut für Quantenoptik, 85748 Garching, Germany
E-mail: sven.hoefling@physik.uni-wuerzburg.de

New Journal of Physics **14** (2012) 083001 (12pp)
Received 23 January 2012
Published 2 August 2012
Online at http://www.njp.org/
doi:10.1088/1367-2630/14/8/083001

Abstract. We report on in-lab free space quantum key distribution (QKD) experiments over 40 cm distance using highly efficient electrically driven quantum dot single-photon sources emitting in the red as well as near-infrared spectral range. In the case of infrared emitting devices, we achieve sifted key rates of 27.2 kbit s^{-1} (35.4 kbit s^{-1}) at a quantum bit error rate (QBER) of 3.9% (3.8%) and a $g^{(2)}(0)$ value of 0.35 (0.49) at moderate (high) excitation. The

[6] These authors have contributed equally to this work.
[7] Present address: Institut für Festkörperphysik, Technische Universität Berlin, 10623 Berlin, Germany.
[8] Author to whom any correspondence should be addressed.

red emitting diodes generate sifted keys at a rate of 95.0 kbit s^{-1} at a QBER of 4.1% and a $g^{(2)}(0)$ value of 0.49. This first successful proof of principle QKD experiment based on electrically operated semiconductor single-photon sources can be considered as a major step toward practical and efficient quantum cryptography scenarios.

Contents

1. Introduction **2**
2. Electrically driven quantum dot (QD) single-photon sources (SPSs) **3**
2.1. InAs QD SPSs 4
2.2. InP QD SPSs 5
3. QKD system **6**
4. QKD experiment **7**
5. Summary and conclusions **10**
Acknowledgments **10**
References **11**

1. Introduction

In 1984 Bennett and Brassard proposed a key distribution protocol (BB84) that uses the quantum mechanical properties of single-photons to detect eavesdropping attempts [1]. Due to the lack of efficient single-photon sources, almost all quantum key distribution (QKD) experiments, however, have been performed with strongly attenuated lasers [2–4]. For such sources various attacks, e.g. number splitting or beam splitting attacks, become possible. Using decoy methods [5], these attacks can be averted but significant shrinking of the sifted key is required. Provided a single-photon source (SPS) with very high efficiency, i.e. with an average number of photons per pulse $\langle n \rangle_{\mathrm{SPS}}$ comparable to average intensities typically used for decoy protocols (e.g. $\langle n \rangle_{\mathrm{dec}} = 0.4$), the reduced protocol overhead gives a clear benefit. Moreover, in the case of a limited number of counts, as expected for future satellite links or other mobile systems, statistical effects arising from the finite key size are far less severe for systems using SPSs [6]. Currently, the maximal detection rates of commercially available single-photon detectors are limited to MHz, while the repetition rates of modern QKD systems steadily increase to the GHz range [7–9]. Therefore high-transmission QKD systems can easily be limited by the receiver. In this case using a SPS even with moderate efficiency will increase the secret key rate. To date, QKD experiments using optically pumped SPSs have been demonstrated with single-nitrogen-vacancy color centers in a diamond nanocrystal (NV-centers) in free space [10, 11] as well as with quantum dots (QDs) in free space [12, 13] or optical fibers [14–16]. These experiments affirmed their great potential for QKD. However, they have of course suffered from drawbacks of the rather inefficient and impractical optical excitation scheme.

In this paper, we report on proof of concept QKD experiments using two different electrically driven QD SPSs emitting in the near-infrared and red spectral range based on InAs and InP QDs, respectively. The infrared emitting devices generate sifted key rates of 27.2 kbit s^{-1} (35.4 kbit s^{-1}) at a quantum bit error rate (QBER) of 3.9% (3.8%) and a $g^{(2)}(0)$

value of 0.35 (0.49) at moderate (high) excitation. In the case of the red emitting diodes we achieve sifted keys at a rate of 95.0 kbit s^{-1}, a QBER of 4.1% and a $g^{(2)}(0)$ value of 0.49.

Whereas wavelengths in the 1.3 and 1.55 μm telecommunication windows are often used for long-distance fiber-based transmission, the shorter wavelengths of our sources have the advantage of being well suited for free space communication. This is due to the fact that Earth's atmosphere has a high-transmission window around 770 nm and thus naturally provides a low-loss communication channel, which is only weakly dispersive and non-birefringent [17]. In addition, the shorter wavelengths utilized in this experiment permit the application of silicon avalanche photo diodes (Si APDs) as detectors with the InP QDs' emission (approx. 650 nm) almost perfectly matching the maximum detection efficiency at about 700 nm. Si APDs also have advantages in terms of higher efficiencies, lower dark count rates and lower afterpulsing probabilities compared to telecom-wavelength InGaAs APDs and easier handling with respect to superconducting single-photon detectors. Particularly large photon extraction efficiencies are achieved for the InAs-based SPSs by exploiting the Purcell effect in a highly optimized micropillar cavity design. Therefore the lower detection efficiency of photons compared to the InP QDs can partly be compensated for. Although both QD SPSs were used in a free space approach in this work, it is worth mentioning that the InAs QD emission (approx. 900 nm) would also allow for short-distance communication in standard telecom fiber as proposed by P D Townsend [18], a fact highlighting the flexibility of QD-based SPSs for quantum cryptography applications. Both device approaches have recently proven their potential, acting as efficient SPSs under pulsed electrical current injection featuring high single-photon emission rates and strong suppression of multiphoton emission events [19, 20] and thus provide an excellent technology platform for the implementation of QKD experiments.

2. Electrically driven quantum dot (QD) single-photon sources (SPSs)

QD SPSs suitable for the QKD experiments were identified using micro-electroluminescence (μEL) together with photon autocorrelation measurements at cryogenic temperatures. In the case of SPSs based on InAs QDs, described in this section, a temperature control assembly additionally allowed for resonance tuning of the single QD emission with respect to the fundamental cavity mode of the micropillar. The samples were excited by electrical pulse generators providing pulses with widths down to 100 ps (full-width at half-maximum (FWHM)) and repetition rates of up to 3.35 GHz. In addition, a DC-offset could be applied to the samples. The μEL from InAs/InP QDs was collected by a $\times 20/\times 50$ microscope objective with a numerical aperture of 0.40/0.45 and spectrally analyzed by a grating monochromator with an attached liquid nitrogen/Peltier cooled Si charge-coupled device (CCD) camera enabling a spectral resolution of about 35 μeV/200 μeV, respectively. Single-photon emission was probed using a Hanbury Brown and Twiss (HBT) setup, which was placed behind the exit slit of the monochromator. The HBT was equipped with single-photon counting modules based on Si APDs with a temporal resolution of approximately 700/500 ps in the case of InAs/InP QDs. $g^{(2)}(0)$ values in this work were evaluated by directly integrating the measured coincidences of the zero delay peak over one full pulse duration and dividing this sum by the mean value of the remaining peaks. We did not apply any corrections, such as background subtraction, to the measured data. In this way, we are giving an upper limit for the two-photon emission probability within the quantum channel.

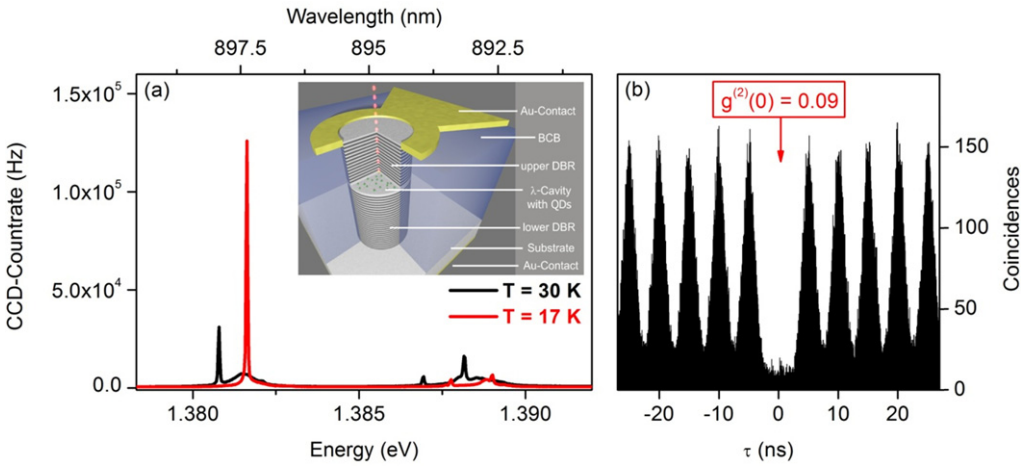

Figure 1. (a) μEL spectra of a QD SPS with a diameter of 2.0 μm at pulsed electrical excitation at 199 MHz. At a temperature of 17 K a single QD line was tuned into resonance with the fundamental cavity mode. Inset: schematic view of an electrically contacted SPS emitting in the near-infrared spectral range. (b) Photon autocorrelation measurement carried out on the SPS signal displayed in (a) at 17 K, revealing a particular pure single-photon emission with $g^{(2)}(0) = 0.09$.

2.1. InAs QD SPSs

The electrically driven SPS emitting in the near-infrared spectral range (see the inset of figure 1(a)) utilized in the QKD system was based on a doped planar microcavity structure grown by molecular beam epitaxy on an n-doped GaAs substrate. The microcavity consists of a 1λ thick undoped GaAs cavity embedded between a lower n-doped distributed Bragg reflector (DBR) and an upper p-doped DBR composed of $\lambda/4$ thick AlAs/GaAs mirror layers. Three-dimensional finite-difference time-domain modeling was performed in order to determine the optimum number of 13/26 mirror pairs in the upper/lower DBR for high extraction efficiency and highly directional emission away from the sample surface [19]. In the vicinity of the low-density InAs QD layer, located at the center of the GaAs cavity, an n-type (δ-doped) layer was introduced to eliminate dark-state configurations that are known to reduce the efficiency of SPSs based on neutral QDs [21]. Thus, electron–hole pair capture owing to electrical excitation predominantly created charged excitons in a singlet configuration, leading to fast recombination of the optically bright excitonic state. For details of the fabrication of electrically contacted micropillars, see [22].

Figure 1(a) displays μEL spectra of a micropillar with a diameter of $d_C = 2.0\,\mu$m operated at a repetition rate of 199 MHz. The device was biased with a dc voltage V_{DC} of 1.450 V, just below the onset of EL. In addition, pulses with an amplitude V_{AC} of 5.25 V were applied. At 30 K, a dominant single QD exciton line as well as the fundamental cavity mode C with a Q-factor of about 2100 can be identified. By decreasing the temperature to 17 K, the X^--line was tuned into resonance with the cavity mode, which resulted in an enhancement of the emission due to the Purcell effect. On resonance, a maximum detection rate of 1.26×10^5 Hz was obtained. As can already be seen from this on-resonance spectrum, this device features a very

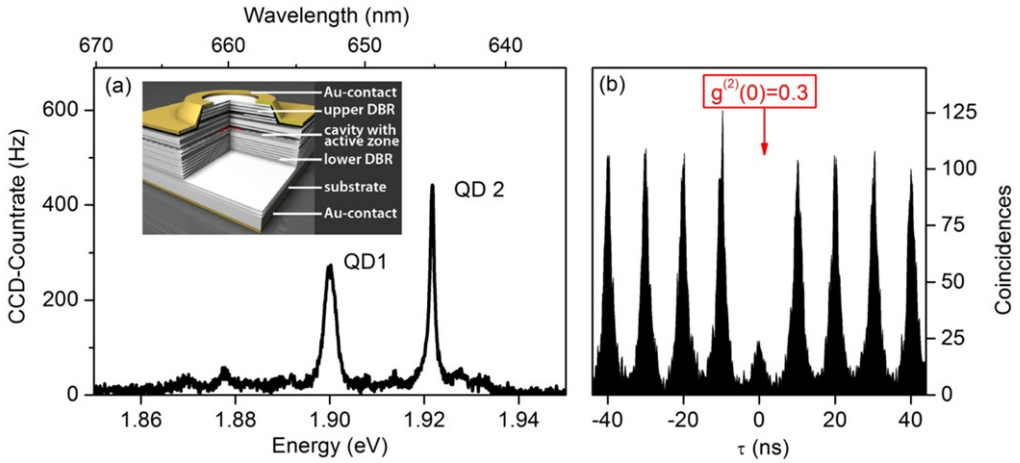

Figure 2. (a) μEL spectrum recorded at 4 K. The emission lines of two different quantum dots (QD1 and QD2) were observable. The charge carrier injection was performed by a dc bias of 2.12 V and an additional pulse with 250 ps FWHM and an amplitude of 2.73 V at a repetition rate of 100 MHz. Inset: illustration of the electrically driven SPS emitting in the red spectral range. (b) The photon autocorrelation measurement associated with QD1 indicates a strong multiphoton suppression with $g^{(2)}(0) = 0.3$.

clean emission spectrum with low background contributions from the fundamental and higher order cavity modes, which are typically fed non-resonantly by spectator QDs in high Q-factor microcavities [23–25]. The photon autocorrelation measurement shown in figure 2(b) confirms the purity of single-photon emission with $g^{(2)}(0) = 0.09$, i.e. with a very low probability of multiphoton emission events, under pulsed electrical operation. It is also worth mentioning that the change in overall performance of this device was below 20% in terms of signal intensity over a period of a few months (including many cool-down and warm-up cycles), which highlights the durability of these devices.

2.2. InP QD SPSs

The SPS emitting in the red spectral range was grown by metal organic vapor phase epitaxy (MOVPE) using standard sources (trimethylgallium, trimethylindium, trimethyl-aluminum, carbon-tetrabromide, dimethylzinc, silane, arsine and phosphine) on a doped (100) GaAs substrate tilted 6° toward the (111)A direction. Self-assembled InP QDs were grown between two $Ga_{0.51}In_{0.49}P$ barriers. This active region is again embedded in a 1λ cavity consisting of two DBRs to enhance the collection efficiency [26]. The bottom DBR consists of 45 $\lambda/4$ layers of Si-doped $AlAs/Al_{0.5}Ga_{0.5}As$, while eight layer pairs of C-doped $Al_{0.5}Ga_{0.5}As/Al_{0.95}Ga_{0.05}As$ constitute the top DBR. Mesas with diameters of about 100 μm were fabricated by common semiconductor photolithography processing steps and wet as well as dry chemical etching. A layer of $(Al_{0.98}Ga_{0.02})_{0.51}In_{0.49}P$ inserted in the upper DBR was oxidized to act as an aperture and mold the flow of current and light. Finally, Au-based ohmic contacts were evaporated for electrical excitation. The whole device structure (illustrated in the inset of figure 2(a)) was mounted on a high-frequency holder terminated with a 50 Ω resistor to avoid back reflection of the electrical signal.

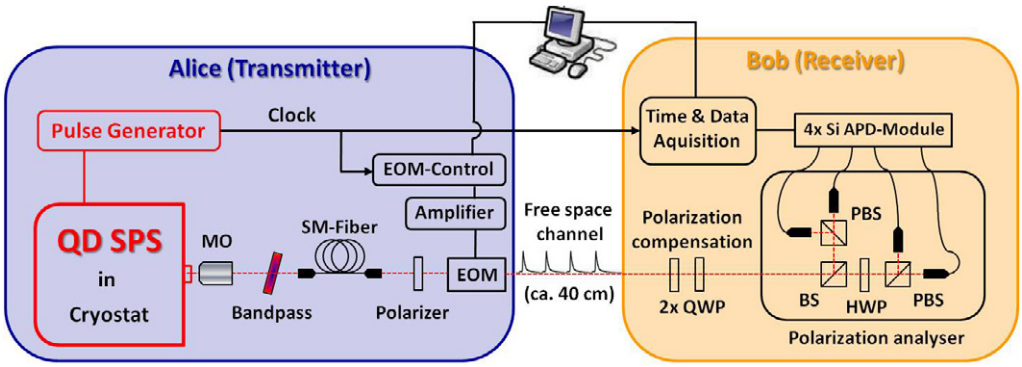

Figure 3. Schematic diagram of the QKD system based on the BB84 protocol with a free space communication channel. The core of the transmitter module was a QDSPS. The latter was electrically triggered by a pulse generator, which acted as clock for the QKD setup. MO—microscope objective, SM—single mode, EOM—electro optic modulator, BS—beam splitter, PBS—polarizing beam splitter, HWP—halve wave plate, QWP—quarter wave plate and APD—avalanche photo diode.

Figure 2(a) shows a μEL spectrum of the used sample under pulsed electrical excitation. A dc bias of 2.12 V and pulses of 2.73 V were applied to the device to inject charge carriers. The repetition rate and the pulse width were fixed at 100 MHz and 250 ps. Emission lines from two different QDs at 1.90 and 1.92 eV with a line width of 2.5 and 1.2 meV, respectively, were observable. For the QKD experiment in section 4 the emission from QD1 was selected due to lower $g^{(2)}(0)$ values at higher excitation power (data not shown) and its brighter emission. For high excitation pulse amplitudes and 200 MHz repetition rate a maximum true single-photon rate ($g^{(2)}(0) < 0.5$) exceeding 350 kHz was achieved on the detectors. This corresponds to a single-photon emission rate of approx. 7 MHz into the acceptance cone of the first lens (NA = 0.45). The photon autocorrelation measurement displayed in figure 2(b) stemmed from QD1 in the μEL spectrum in panel (a). The suppression of multiphoton emission by a factor of 3.3 indicates that the QD is a true single-photon emitter. The non-vanishing $g^{(2)}(0)$ value can be explained by uncorrelated background emission and recapture processes due to the finite length of the excitation pulse.

3. QKD system

The experimental setup of the QKD system is shown in figure 3. As the core of the transmitter module (Alice), the respective SPS presented in the previous section was mounted on the cold finger of a liquid He flow-type cryostat and excited by an electrical pulse generator (cf section 2). The QD emission was collected by a microscope objective, spectrally filtered by an interference bandpass filter, and coupled into a single-mode optical fiber (780HP/SM600 for InAs/InP-QDs). The use of narrow interference bandpass filters (FWHM of 0.25 /1 nm for InAs/InP-QDs) instead of a monochromator significantly simplifies the setup. Single-photon emission was probed using a fiber-coupled HBT setup with Si APDs acting as detectors.

Additionally, the SPS emission could be monitored by a monochromator with an attached CCD.

For the actual QKD experiment the fiber-coupled SPS signal was polarized and the four polarization states for the BB84 protocol were set by a fast electro-optic modulator (EOM) (here we used horizontal and vertical linear polarizations together with right and left circular polarizations). In this proof of concept experiment, we were only interested in the key parameters of our system, i.e. sifted key rate and error rate. Therefore the EOM was controlled by a waveform generator with a fixed, repeating pattern of the four polarization states. After the EOM photons left the transmitter and propagated through a short free space link to the receiver module (Bob). Two quarter wave plates were used to rotate the circular polarizations to $\pm 45^{\circ}$ linear polarizations and align the horizontal and vertical axes of the transmitter and the receiver. The photons then entered the polarization analyzer where the measurement basis was chosen randomly using a beam splitter. The photons were detected by four Si APDs connected to the data acquisition electronics. The whole setup was synchronized using the pulse generator's trigger output as a global clock. The detection events were transferred to a computer performing time filtering and key sifting. The maximum repetition rate $f_{\max}$ of the system is limited to 200 MHz by the EOMs bandwidth, but the achievable detection rate is limited to 4 MHz by the commercial APD modules. Thus, for any system for which the product $f_{\max} \times \langle n \rangle_{\mathrm{SPS}} \times \tau \times \eta$, where τ is the transmission of the link and η is the efficiency of the detectors, exceeds this maximum rate, SPSs have a clear advantage.

4. QKD experiment

The first QKD experiment used the near-infrared emitting InAs-based SPS ($\lambda \approx 897$ nm) described in section 2.1. Figure 4(a) shows the on-resonance μEL spectrum ($T = 20$ K) recorded with the spectrometer (repetition rate $f = 182.6$ MHz).

For optimum performance regarding emission intensity and signal-to-background ratio, the excitation parameters $V_{\mathrm{DC}} = 1.400\,V$ and $V_{\mathrm{AC}} = 6.0$ V were chosen. In order to measure the purity of single-photon emission inside the quantum channel, the bandpass filtered μEL signal of figure 4(a) was directly coupled to the HBT setup. The resulting photon autocorrelation function is depicted in figure 4(b), revealing a $g^{(2)}(0)$ value of $0.35 < 0.5$ as a clear signature of single-photon emission. The fact that we observed higher values of $g^{(2)}(0)$ compared to measurements with a monochromator is mainly due to the finite bandwidth of the interference filter, which causes increased contributions of uncorrelated background emission.

In order to perform the QKD experiment, the bandpass filtered single-photon emission was coupled into a single mode fiber connected to the transmitter module described in section 3. The excitation conditions remained unchanged except for the dc-offset V_{DC} which served as control parameter for the single-photon emission rate (as reported in [19]). Figure 5 summarizes the recorded sifted key rates, QBER and $g^{(2)}(0)$ values.

For a low excitation at $V_{\mathrm{DC}} = 1.350\,V$ we measured a sifted key rate of 8.6 kbit s^{-1} at $g^{(2)}(0) = 0.30$. The sifted key rate increased up to 27.2 kbit s^{-1} at $V_{\mathrm{DC}} = 1.400\,V$ and a slightly higher $g^{(2)}(0)$ value of 0.35 (cf figure 4(a)). Further increasing V_{DC}, the sifted key rate finally saturated due to QD saturation accompanied by a noticeable rise in the $g^{(2)}(0)$ value. The latter can be explained by increasing contributions of uncorrelated background emission from the cavity mode. Figure 5(b) affirms that the sifted key rates were recorded at a low level of the

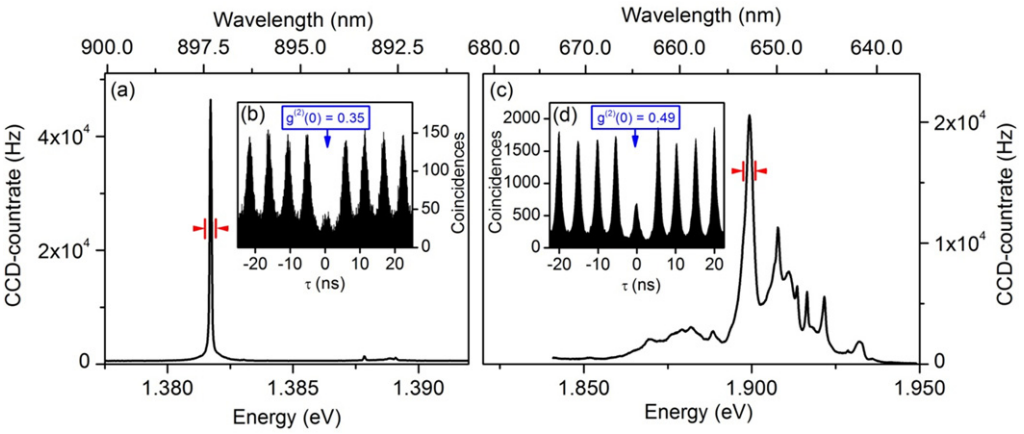

Figure 4. (a) μEL spectrum of a QD micropillar SPS emitting in the near-infrared spectral range under pulsed electrical excitation at 182.6 MHz. The red arrows indicate spectral filtering by a 0.25 nm interference bandpass filter. (b) Photon autocorrelation measurement carried out on the SPS signal in (a), where the bandpass filtered emission was directly coupled to the HBT setup. The $g^{(2)}(0)$ value of 0.35 clearly prooves single-photon emission with a strong suppression of multiphoton emission events. (c) μEL spectrum of the resonant cavity diode structure emitting in the red spectral range. Charge carrier injection was performed by electrical pulses with a repetition rate of 200 MHz. The red arrows display spectral filtering by a 1 nm interference bandpass filter. (d) Photon autocorrelation measurement of the spectrally filtered signal of (c) using a fiber-coupled HBT setup with a temporal resolution of 500 ps.

QBERs. In fact, the QBER drops from 5.3% at low excitation to values of roughly 4% owing to the increasing signal to background ratio, which was already close to the contrast limit of the EOM ($\approx 3\%$). Increasing the excitation, even higher sifted key rates of up to 35.4 kbit s^{-1} at $g^{(2)}(0) = 0.49$ could be obtained at the cost of higher $g^{(2)}(0)$ values—a trend that is illustrated in figure 5(c). The corresponding QBERs were in the range of 3.8–6.7%.

The second QKD experiment was performed using the InP-based resonant cavity light-emitting diode emitting at about 650 nm. Along the lines of section 2.2 a fixed bias of 2.12 V was applied to the device just below the onset of EL and additional pulses of 250 ps pulse width and amplitudes from 2.71 up to 3.86 V accomplished the carrier injection into the active region. In order to achieve higher emission rates, the repetition rate was raised to 200 MHz, only restricted by the maximum EOM frequency. The μEL spectrum for 3.71 V pulse amplitude is shown in figure 4(c) where the red arrows display spectral filtering, and figure 4(d) shows the corresponding photon autocorrelation measurement indicating the suppression of multiphoton emission via the $g^{(2)}(0)$ value of 0.49.

The sifted key rates, $g^{(2)}(0)$ values and QBERs of the pulse amplitude series are displayed in figures 6(a) and (b). Due to the increased injection of charge carriers into the QD the sifted key rate increased from 9.2 kbit s^{-1} up to 117 kbit s^{-1}. As an undesirable effect the background emission also increased and consequently downgraded the single-photon emission quality observable via an increase of the $g^{(2)}(0)$ value. The QBER dropped from 6% down to

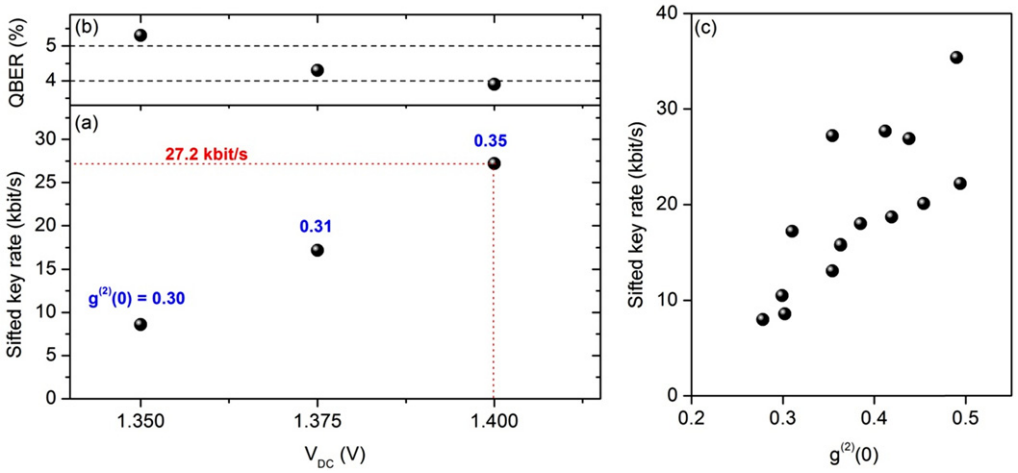

Figure 5. QKD data achieved with an electrically driven QD micropillar SPS emitting in the near-infrared spectral range ($f = 182.6$ MHz): (a) and (b) sifted key rates, QBER and the corresponding $g^{(2)}(0)$ values (in blue) as a function of the parameter V_{DC}. The dashed red line indicates the data corresponding to the measurement displayed in figures 4(a) and (b). (c) Sifted key rate as a function of the $g^{(2)}(0)$ value.

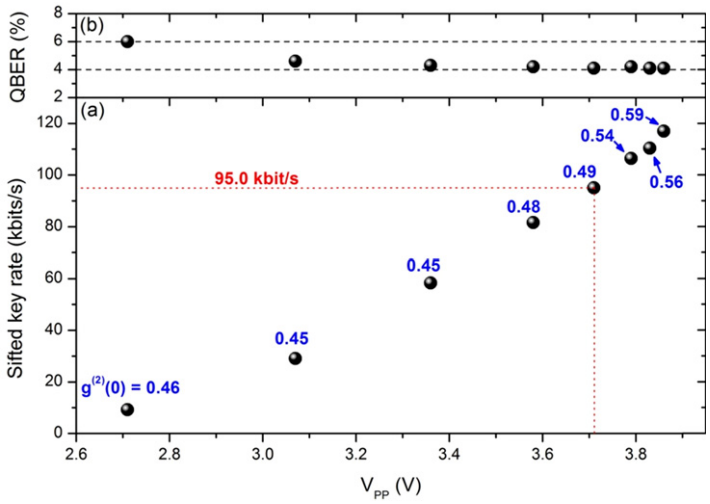

Figure 6. (a) Sifted key rates, $g^{(2)}(0)$ values (in blue) and (b) QBERs achieved with the presented QKD experiment and the red emitting SPS at a repetition frequency of 200 MHz. The higher the pulse amplitudes applied, the higher the sifted key rates achieved. The $g^{(2)}(0)$ values, however, also increased because of the upcoming background contribution. Almost all QBERs were below 5%. The dashed red line indicates the data corresponding to the measurement presented in figures 4(c) and (d).

nearly 4% comparable to the results discussed above. The highest sifted rate with $g^{(2)}(0) < 0.5$ was 95.0 kbit s^{-1}, achieved at an excitation pulse amplitude of 3.71 V (cf the dashed red line in figure 6(a)).

Table 1. Results of the QKD experiment performed with the two different electrically operated QD SPSs: sifted key rate (SKR), QBER and corresponding $g^{(2)}(0)$ values for three different pumping conditions.

	Low pumping			Moderate pumping			High pumping		
λ (nm)	SKR (kbit s^{-1})	QBER (%)	$g^{(2)}(0)$	SKR (kbit s^{-1})	QBER (%)	$g^{(2)}(0)$	SKR (kbit s^{-1})	QBER (%)	$g^{(2)}(0)$
897	8.0	6.7	0.28	27.2	3.9	0.35	35.4	3.8	0.49
653	9.2	6.0	0.46	95.0	4.1	0.49	117.0	4.1	0.59

In our experiment the detection rates of about 200 kHz are below the maximum detection rates of 4 MHz by about a factor of 20. However, improvements of the coupling of photons into single mode fibers and particularly the development of cavities containing only a single QD should make the required increase feasible, likely enabling SPS systems to outperform attenuated pulse systems. In particular, lower $g^{(2)}(0)$ values will lead to higher achievable communication distances (or channel losses) as outlined in [27].

5. Summary and conclusions

For the first time, the utilization of electrically driven QD SPSs emitting in the red as well as infrared spectral range for QKD was evaluated. The main results are summarized in table 1.

Emulating a BB84 protocol we achieve a sifted key rate of 27.2 kbit s^{-1}(35.4 kbit s^{-1}) at a QBER of 3.9% (3.8%) and a $g^{(2)}(0)$ value of 0.35 (0.49) with the infrared emitting device ($\lambda \approx 897$ nm) at moderate (high) excitation. With the red emitting diode ($\lambda \approx 653$ nm) sifted keys could be generated at a rate of 95.0 kbit s^{-1} with a QBER of 4.1% and a $g^{(2)}(0)$ value of 0.49. The fact that we achieve higher sifted key rates with the InP-based SPS is mainly due to the higher detection efficiency of the Si APDs in the red spectral range. The second trend, that we observe at general lower $g^{(2)}(0)$ values for the InAs QD SPS results from a stronger suppression of uncorrelated background contributions in this device if compared to InP-based SPS (cf figure 4). This is especially evident for the low excitation regime where we observe $g^{(2)}(0)$ values as low as 0.28 for the infrared emitting device. Therefore, by following the InAs as well as InP material approach we cover the benefits of both systems in this work, which highlights the flexibility of QD-based SPSs for quantum cryptography applications. We believe that this successful QKD proof of concept of two different electrically operated semiconductor SPSs can be considered to be a major step toward practical and efficient QKD scenarios. With new technological developments like positioned single QDs inside the micropillar resonator [28, 29] and more efficient output coupling, we expect key rates outperforming attenuated pulse QKD systems.

Acknowledgments

This work was financially supported by the German Ministry of Education and Research through the projects QPENS and EPHQUAM. Expert sample preparation by M Emmerling and A Wolf is gratefully acknowledged.

References

[1] Bennett C H and Brassard G 1984 Quantum cryptography: public key distribution and coin tossing *Proc. IEEE Int. Conf. on Computers Systems and Signal Processing* (*Bangalore, India*) pp 175–9

[2] Ali S, Saharudin S and Wahiddin M R B 2009 Implementation of decoy state protocol *Eur. J. Sci. Res.* **33** 183–6

[3] Chen T-Y *et al* 2009 Field test of a practical secure communication network with decoy-state quantum cryptography *Opt. Express* **17** 6540

[4] Zhao Y, Qi B, Ma X, Lo H-K and Qian L 2006 Experimental quantum key distribution with decoy states *Phys. Rev. Lett.* **96** 070502

[5] Wang X-B 2005 Beating the photon-number-splitting attack in practical quantum cryptography *Phys. Rev. Lett.* **94** 230503

[6] Scarani V, Behmann-Pasquinucci H, Cerf N J, Dušek M, Lütkenhaus N and Peev M 2009 The security of practical quantum key distribution *Rev. Mod. Phys.* **81** 1301

[7] Gordon K J, Fernandez V, Buller G S, Rech I, Cova S D and Townsend P D 2005 Quantum key distribution system clocked at 2 GHz *Opt. Express* **13** 3015–20

[8] Namekata N, Takesue H, Honjo T, Tokura Y and Inoue S 2011 High-rate quantum key distribution over 100 km using ultra-low-noise, 2 GHz sinusoidally gated InGaAs/InP avalanche photodiodes *Opt. Express* **19** 10632–9

[9] Dixon A R, Yuan Z L, Dynes J F, Sharpe A W and Shields A J 2010 Continuous operation of high bit rate quantum key distribution *Appl. Phys. Lett.* **96** 161102

[10] Beveratos A, Brouri R, Gacoin T, Villing A, Poizat J-P and Grangier P 2002 Single photon quantum cryptography *Phys. Rev. Lett.* **89** 187901

[11] Alleaume R, Treussart F, Messin G, Dumeige Y, Roch J-F, Beveratos A, Brouri-Tualle R, Poizat J-P and Grangier P 2004 Experimental open-air quantum key distribution with a single-photon source *New J. Phys.* **6** 92

[12] Waks E, Inoue K, Santori C, Fattal D, Vuckovic J, Solomon G S and Yamamoto Y 2002 Quantum cryptography with a photon turnstile *Nature* **420** 762

[13] Aichele T, Reinaudi G and Benson O 2004 Separating cascaded photons from a single quantum dot: demonstration of multiplexed quantum cryptography *Phys. Rev.* B **70** 235329

[14] Intallura P M, Ward M B, Karimov O Z, Yuan Z L, See P, Atkinson P, Ritchie D A and Shields A J 2009 Quantum communication using single photons from a semiconductor quantum dot emitting at a telecommunication wavelength *J. Opt.* A **11** 054005

[15] Collins R J *et al* 2010 Quantum key distribution system in standard telecommunications fiber using a short wavelength single photon source *J. Appl. Phys.* **107** 073102

[16] Takemoto K *et al* 2010 Transmission experiment of quantum keys over 50 km using high-performance quantum-dot single-photon source at 1.5 μm wavelength *Appl. Phys. Express* **3** 092802

[17] Gisin N, Ribordy G, Tittel W and Zbinden H 2002 Quantum cryptography *Rev. Mod. Phys.* **74** 145–95

[18] Townsend P D 1998 Experimental investigation of the performance limits for first telecommunications-window quantum cryptography systems *IEEE Photonics Technol. Lett.* **10** 1048–50

[19] Heindel T, Schneider C, Lermer M, Kwon S H, Braun T, Reitzenstein S, Höfling S, Kamp M and Forchel A 2010 Electrically driven quantum dot-micropillar single photon source with 34% overall efficiency *Appl. Phys. Lett.* **96** 011107

[20] Reischle M, Kessler C, Schulz W-M, Eichfelder M, Roßbach R, Jetter M and Michler P 2010 Triggered single-photon emission from electrically excited quantum dots in the red spectral range *Appl. Phys. Lett.* **97** 143513

[21] Strauf S, Stoltz N G, Rakher M T, Coldren L A, Petroff P M and Bouwmeester D 2007 High-frequency single-photon source with polarization control *Nature Photonics* **1** 704–8

[22] Böckler C *et al* 2008 Electrically driven high-Q quantum dot-micropillar cavities *Appl. Phys. Lett.* **92** 091107

[23] Press D, Götzinger S, Reitzenstein S, Hofmann C, Löffler A, Kamp M, Forchel A and Yamamoto Y 2007 Photon antibunching from a single quantum-dot-microcavity system in the strong coupling regime *Phys. Rev. Lett.* **98** 117402

[24] Hennessy K, Badolato A, Winger M, Gerace D, Atature M, Gulde S, Fält S, Hu E L and Imamoglu A 2007 Quantum nature of a strongly coupled single quantum dot-cavity system *Nature* **445** 896–9

[25] Ates S, Ulrich S M, Ulhaq A, Reitzenstein S, Löffler A, Höfling S, Forchel A and Michler P 2009 Non-resonant dot-cavity coupling and its potential for resonant single-quantum-dot spectroscopy *Nature Photonics* **3** 724–8

[26] Schulz W-M, Eichfelder M, Reischle M, Kessler C, Roßbach R, Jetter M and Michler P 2011 Pulsed single-photon resonant-cavity quantum dot LED *J. Cryst. Growth* **315** 127–30

[27] Waks E, Santori C and Yamamoto Y 2002 Security aspects of quantum key distribution with sub-Poisson light *Phys. Rev.* A **66** 042315

[28] Schneider C, Heindel T, Huggenberger A, Weinmann P, Kistner C, Kamp M, Reitzenstein S, Höfling S and Forchel A 2009 Single photon emission from a site-controlled quantum dot-micropillar cavity system *Appl. Phys. Lett.* **94** 111111

[29] Schneider C, Heindel T, Huggenberger A, Niederstrasser T A, Reitzenstein S, Forchel A, Höfling S and Kamp M 2012 Microcavity enhanced single photon emission from an electrically driven site-controlled quantum dot *Appl. Phys. Lett.* **100** 091108